[7]G. M. Raisbeck and T. D. Thomas, Phys. Rev. 172, 1272 (1968).
[8]H. W. Schmitt, J. H. Neiler, F. J. Walter, and A. Chetham-Strode, Phys. Rev. Letters 9, 427 (1962).
[9]M. Asghar, C. Carles, R. Chastel, T. P. Doan, M. Ribrag, and C. Signarbieux, Nucl. Phys. A145, 657 (1970).
[10]C. Carles, M. Asghar, T. P. Doan, R. Chastel, and C. Signarbieux, in *Proceedings of the Second International Atomic Energy Symposium on Physics and Chemistry of Fission, Vienna, Austria, 1969* (International Atomic Energy Agency, Vienna, Austria, 1969).
[11]C. Carles, Ph.D. thesis, University of Bordeaux (unpublished).
[12]B. T. Geilikman and G. I. Khlebnikov, Atom. Energ. (USSR) 18, 218 (1965) [transl.: Soviet J. At. Energy 18, 274 (1965)].
[13]Y. Boneh, Z. Fraenkel, and I. Nebenzahl, Phys. Rev. 156, 1305 (1967).
[14]A. Katase, J. Phys. Soc. Japan 25, 933 (1968).
[15]P. Fong, Phys. Rev. C 2, 735 (1970).
[16]J. R. Nix, Nucl. Phys. A130, 241 (1969).
[17]I. Balla and G. Ben-David, Nucl. Instr. Methods 33, 306 (1965).
[18]N. A. Perfilov and Z. L. Solov'eva, Zh. Eksperim. i Teor. Fiz. 37, 1157 (1959) [transl.: Soviet Phys.—JETP 10, 825 (1960)].
[19]R. A. Atneosen, T. A. Thomas, and G. T. Garvey, Phys. Rev. 139, B307 (1965).
[20]T. D. Thomas and S. L. Whetstone, Phys. Rev. 144, 1060 (1966).
[21]S. W. Cosper, J. Cerny, and R. C. Gatti, Phys. Rev. 154, 1193 (1967).
[22]H. W. Schmitt, J. H. Neiler, and F. J. Walter, Phys. Rev. 141, 1146 (1966).
[23]E. Nardi, Y. Gazit, and S. Katcoff, Phys. Rev. 182, 1244 (1969).
[24]J. Terrell, Phys. Rev. 127, 880 (1962).
[25]E. Nardi and Z. Fraenkel, Phys. Rev. Letters 220, 1248 (1968); Phys. Rev. C 2, 1156 (1970).
[26]E. Cheifetz and Z. Fraenkel, Phys. Rev. Letters 21, 36 (1968).

PHYSICAL REVIEW C VOLUME 4, NUMBER 1 JULY 1971

Form Factors for Proton Transfer Reactions to Unbound Isobaric Analog States*

S. A. A. Zaidi and W. R. Coker
Center for Nuclear Studies, University of Texas, Austin, Texas 78712
(Received 18 January 1971)

Proton form factors for isobaric analog resonances populated directly as residual states in (d,n) and $(^3\mathrm{He},d)$ reactions are discussed and computed explicitly using a Lane-model Hamiltonian and the formalism of Feshbach's unified reaction theory. The resonance form factors thus obtained are compared in specific cases with equivalent parent bound-state form factors and with single-particle resonance wave functions. Numerical results and tests using data are presented for $^{92}\mathrm{Mo}(d,n)^{93}\mathrm{Tc}^A$, and it is shown that resonance form factors lead to a dramatic enhancement of the magnitude of the calculated cross section for some transitions, compared with calculations using conventional form factors. Such enhancements are consistent with the available data.

I. INTRODUCTION

Reactions populating residual nuclear states unbound to particle emission are attractive from both experimental and theoretical viewpoints, and a large number of investigations have been concerned with such reactions. A theoretical study of direct reactions populating single-particle resonances with widths of $\lesssim$100 keV has been made by Levin.[1] Later work by Bunakov,[2] and Vincent and Fortune[3] has dealt with the problems raised by the slow numerical convergence of the distorted-wave Born-approximation (DWBA) transition amplitude when the usual bound-state form factor is replaced by a single-particle resonance continuum form factor. Huby[4] has discussed possible approximations for stripping reactions to "pseudo-bound" states, i.e., states unbound by a few hundred keV.

Interest has been spurred recently in such analyses, by the increasing availability of data,[5,6] particularly for population by direct proton transfer reactions of isobaric analog resonances (IAR) in medium to heavy nuclei.[7-9] However, analysis of direct reactions populating IAR involves certain problems which have received little attention in the literature to date.

Although nuclear forces are charge-independent to a very good approximation, the total nuclear Hamiltonian contains the Coulomb potential energy and various charge-dependent effective nuclear interactions. If one is interested in the wave functions of various members of an isobaric multiplet, such isospin-violating terms in the Hamiltonian cannot be ignored. Use of the isospin raising and lowering operators $T_\pm$ to connect members of an isobaric multiplet implies the space part of their

state functions to be identical.

Thus if Φ_n is the state function of a bound neutron in a medium to heavy nucleus, the state function of its ideal isobaric analog is

$$\chi_p^A = T_-(\Phi_n),$$

which we shall call approximation (A). In fact the actual analog resonance wave function χ_p^R has approximately the same radial shape as Φ_n only in the nuclear interior. Since Φ_n is bound while χ_p^R is a continuum state, the approximation $\chi_p^R \approx \chi_p^A$ begins to break down in precisely the most critical region for a direct reaction, the nuclear surface region.

Such difficulties have already been encountered in analysis of (^{3}He, d) and (d, n) reaction data for IAR in the mass-90 region,[7-9] where if approximation (A) is used, anomalous enhancements of 3 to 5 in the experimental cross sections for $l=2$ transitions over the DWBA cross sections are reported.[8]

A simple alternate approach is to use as a form factor a continuum wave function for a Woods-Saxon potential adjusted to have a resonance at the observed energy of the IAR. However, such a form factor does not in general satisfy approximation (A) in the nuclear interior, except accidentally. In the potential resonance approach such departures from Φ_n within the nucleus are arbitrary and parameter-sensitive. However, such departures are dependent, in a theory of IAR, on isospin mixing, for example, and thus have considerable significance. Moreover, if there is an angular momentum mismatch, calculations involving potential resonance form factors may not be very reliable.[7, 9, 10] Finally, the normalization of such a form factor is ambiguous.

In what follows, we show how to calculate the wave function of an IAR in Lane's model[11, 12] using Feshbach's unified theory of reactions.[13] Such an approach is more useful than solving the Lane coupled equations directly, since we are interested in the explicit energy dependence of the solution, as well as generalizations to include effects arising from mixing of the analog state with surrounding $T_<$ states, and from other modes of decay of the IAR.[14]

We find that the calculated resonance wave function differs significantly from the parent neutron state function, and present numerical results for ^{92}Mo(d, n)Tc^A to the $\frac{5}{2}^+$, $\frac{1}{2}^+$, and $\frac{3}{2}^+$ IAR.

II. WAVE FUNCTION OF THE ISOBARIC ANALOG RESONANCE

We are interested in obtaining the wave function of the resonance state, populated by a proton transfer reaction. This calculation is performed using Lane's model.[11] Subsequently, we will discuss the domain of applicability of this calculation and possible generalizations. The Hamiltonian appropriate to Lane's model may be written as

$$H = H_C + (\tfrac{1}{2}+t_3)K_n + (\tfrac{1}{2}-t_3)K_p + U_O + (\vec{t}\cdot\vec{T})V_1 + (\tfrac{1}{2}-t_3)V_C, \quad (1)$$

where

$$H_C = |C\rangle E_C \langle C| + |A\rangle E_A \langle A|. \quad (2)$$

Here $|C\rangle$ and $|A\rangle$ represent the nuclear ground state and its analog, respectively, of the target nucleus, left behind *after* the proton decay of the IAR. Similarly E_C and E_A are the respective energy eigenvalues of the two states. The isospin operators for the extra nucleon and the core (target) nucleus are denoted by $\vec{t}$ and $\vec{T}$, respectively. The charge-exchange potential, the main term of the optical potential, and the Coulomb potential are denoted, respectively, by V_1, U_O, and V_C. Finally, K_n and K_p are the kinetic energy operators for the neutron and proton, respectively.

To proceed we define two projection operators,

$$P \equiv \int |pC\rangle |\tilde{\phi}_{\epsilon'}\rangle\, d\epsilon' \langle\tilde{\phi}_{\epsilon'}| \langle pC|, \quad (3)$$

and

$$Q \equiv |pC\rangle \sum_{i=1}^{N} |\tilde{\Phi}_p^{(i)}\rangle\langle\tilde{\Phi}_p^{(i)}| \langle pC| + |nA\rangle |\Phi_n\rangle\langle\Phi_n| \langle nA|. \quad (4)$$

The kets $|pC\rangle$ and $|nA\rangle$ stand for the products of the isospin kets for the extra nucleon and the core nucleus. The functions $\tilde{\phi}_\epsilon$, $\tilde{\Phi}_p^{(i)}$, and Φ_n satisfy the following equations:

$$(E_C + K_p + U_O - \tfrac{1}{2}T_0 V_1 + V_C - \Delta - \epsilon)\tilde{\phi}_\epsilon = 0; \quad (5)$$

$$(E_C + K_p + U_O - \tfrac{1}{2}T_0 V_1 + V_C - \Delta - E_p^{(i)})\tilde{\Phi}_p^{(i)} = 0, \quad (i = 1, 2, \ldots, N); \quad (6)$$

$$[E_A + K_n + U_O + \tfrac{1}{2}(T_0 - 1)V_0 - E_n]\Phi_n = 0; \quad (7)$$

$$\langle\tilde{\phi}_\epsilon|\tilde{\phi}_{\epsilon'}\rangle = \delta(\epsilon - \epsilon'), \quad \text{and } \langle\Phi_n|\Phi_n\rangle = 1. \quad (8)$$

Equations (5) and (6) are recognized as the optical-model equations for the scattering and bound states of the proton. The quantity Δ denotes an additional potential that effectively deepens the total potential for the protons.[15] The motivation for this term is as follows: If one deletes the term Δ, Eqs. (5) and (7) are the homogeneous equations obtained from the corresponding coupled Lane equations by dropping the coupling. It is, however, often not noticed that with a realistic choice of optical-model parameters this equation dis-

plays in general a very narrow single-particle resonance far below the Coulomb barrier. This resonance is caused by the proton state which has the same number of nodes and total angular momentum as the neutron orbit of the parent analog state (nC), formed by adding a neutron to the core nucleus. The occurrence of this proton state in the continuum renders the proton continuum manifestly nonorthogonal to the isobaric analog state, if the latter is defined as the state obtained by operating upon the parent analog state with the isospin-lowering operator T_-.

We avoid the complications arising from this nonorthogonality by choosing Δ such that the sharp single-proton resonance is moved to negative energy. The few normalized bound states defined by Eq. (6), and the continuum eigenstates of Eq. (5), subjected to the conditions (8), now define a *complete, orthonormal* set of single-proton states. It now follows that

$$PQ = QP = 0 . \tag{9}$$

In the spirit of the shell-model approach, we now seek an expansion of the solution of Lane's model in terms of the functions $\tilde{\phi}_\epsilon$, $\tilde{\Phi}_p^{(i)}$, and the single function Φ_n discussed above. Thus we write

$$\Psi_E = P\Psi_E + Q\Psi_E . \tag{10}$$

The Schrödinger equation corresponding to the Hamiltonian in (1) is readily solved. One obtains[13]

$$P\Psi_E^{(-)} = \xi^{(-)} + \frac{1}{E^{(-)} - PHP} PHQ \times \frac{1}{E - QHQ - QHP[E^{(-)} - PHP]^{-1}PHQ} QHP\xi^{(-)} , \tag{11}$$

and

$$Q\Psi_E^{(-)} = \frac{1}{E - QHQ - QHP[E^{(-)} - PHP]^{-1}PHQ} QHP\xi^{(-)} , \tag{12}$$

where $\xi^{(-)}$ is a solution of

$$(E^{(-)} - PHP)\xi^{(-)} = 0 . \tag{13}$$

To proceed further, we consider the eigenvalue problem,

$$(E_i - QHQ)\zeta_i = 0 , \quad (i = 1, 2, \ldots, N+1) . \tag{14}$$

This amounts to the diagonalization of H on the bound states $\tilde{\Phi}_p^{(i)}$ and Φ_n. The matrix QHQ has a very simple structure, since the matrix elements connecting the bound proton states involve only the potential Δ. The off-diagonal elements of this part of the matrix are very much smaller than diagonal ones, since the proton functions are mutually orthogonal, and we can take Δ to have a volume shape like U_0. The matrix elements involving the neutron state Φ_n, and the proton state with the same radial (and angular momentum) quantum numbers $\tilde{\Phi}_p^{(1)}$ are large. Finally the matrix elements connecting neutron and proton functions with a different number of nodes are small. The function $\tilde{\Phi}_p^{(1)}$ depends upon the arbitrarily chosen potential Δ; however, for values of Δ lying in the neighborhood of the minimum value of Δ capable of moving the single-proton resonance to negative energy, the functions $\tilde{\Phi}_p^{(1)}$ and Φ_n have essentially the same radial dependence.

The solutions of Eq. (14) and the corresponding eigenvalues have some expected properties. Two eigenvalues E_1 and E_2 lie close to the energy of the IAR and the proton single-particle resonance, respectively. Numerical calculations performed for the IAR in ^{93}Tc show that the corresponding normalized solutions are very well approximated by

$$\zeta_1 \cong \frac{1}{(2T_0+1)^{1/2}}[\,|pC\rangle\tilde{\Phi}_p^{(1)} + \sqrt{2T_0}\,|nA\rangle\Phi_n] , \tag{15}$$

and

$$\zeta_2 \cong \frac{1}{(2T_0+1)^{1/2}}[\sqrt{2T_0}\,|pC\rangle\tilde{\Phi}_p^{(1)} - |nA\rangle\Phi_n] . \tag{16}$$

The approximation involves dropping the small components of the eigenvector due to admixtures of proton wave functions with a lesser number of nodes. The expressions used to approximate ζ_1 and ζ_2 have been derived by several authors using schematic models. A particularly clear derivation is found in Robson.[16] For obvious reasons we shall also denote ζ_1 and ζ_2 by $\zeta_>$ and $\zeta_<$, respectively.[16] Likewise we shall occasionally write $E_>$ and $E_<$ for E_1 and E_2. The other eigenvectors involve almost exclusively linear combinations of proton functions with a lesser number of nodes. The set of eigenvectors $\{\zeta_1\}$ constitutes a basis for the space on which Q projects. Next, we consider the solutions of the eigenvalue equation

$$\left[\mathcal{E}_\mu - QHQ - QHP\frac{1}{E^{(-)} - PHP}PHQ\right]\xi_\mu = 0 . \tag{17}$$

These solutions are needed to obtain a bilinear expansion of the inverse operator in Eqs. (11) and (12). It is convenient to write

$$\Xi_\mu = \sum_\mu a_{\mu\nu}\zeta_\nu , \tag{18}$$

and seek the coefficients $a_{\mu\nu}$ such that Eq. (17) is satisfied. The matrix corresponding to the Eq. (17) is complex and symmetric (and thus non-Hermitian). In addition to Ξ_μ, we introduce the adjoint $\tilde{\Xi}_\mu$ as the solution to

$$\left[\mathcal{E}_\mu^* - QHQ - QHP\frac{1}{E^{(+)} - PHP}PHQ\right]\tilde{\Xi}_\mu = 0 . \tag{19}$$

In terms of these solutions, we obtain

$$P\Psi_E^{(-)} = \xi^{(-)} + \frac{1}{E^{(-)} - PHP} PHQ \sum_\mu \frac{|\Xi_\mu\rangle\langle\tilde{\Xi}_\mu| QHP|\xi^{(-)}\rangle}{E - \mathcal{E}_\mu}, \tag{20}$$

and

$$Q\Psi_E^{(-)} = \sum_\mu \frac{|\Xi_\mu\rangle\langle\tilde{\Xi}_\mu| QHP|\xi^{(-)}\rangle}{E - \mathcal{E}_\mu}. \tag{21}$$

In Eqs. (20) and (21) we now approximate $|\tilde{\Xi}_\mu\rangle$ and $|\Xi_\mu\rangle$ by $|\zeta_\mu\rangle$ and observe that only $|\zeta_>\rangle$ and $|\zeta_<\rangle$ give significant contributions. Numerical calculations show that this is a very good approximation. One can easily show that the following relations are valid:

$$\langle\zeta_>| QHP|\xi^{(-)}\rangle = \frac{1}{(2T_0+1)^{1/2}}\langle\tilde{\Phi}_p^{(1)}|\Delta|\xi^{(-)}\rangle \equiv \left(\frac{\Gamma_>}{2\pi}\right)^{1/2}, \tag{22}$$

$$\langle\zeta_<| QHP|\xi^{(-)}\rangle = \left(\frac{2T_0}{2T_0+1}\right)^{1/2}\langle\tilde{\Phi}_p^{(1)}|\Delta|\xi^{(-)}\rangle \equiv \left(\frac{\Gamma_<}{2\pi}\right)^{1/2}. \tag{23}$$

In Eqs. (22) and (23), we have introduced the complex quantities $\Gamma_>$ and $\Gamma_<$ for convenience. Expanding Green's function $(E^{(-)} - PHP)^{-1}$ in Eqs. (20) and (21), and using Eq. (10), we write the solution finally as

$$\Psi_E^{(-)} = \xi^{(-)} + \frac{(\Gamma_</2\pi)^{1/2}}{E - E'_< - i(\Gamma_</2)}\left[|\zeta_<\rangle + \left(\frac{2T_0}{2T_0+1}\right)^{1/2}\int \frac{|\xi_\epsilon^{(-)}\rangle\langle\xi_\epsilon^{(-)}|\Delta|\tilde{\Phi}_p^{(1)}\rangle d\epsilon}{E^{(-)} - \epsilon}\right]$$
$$+ \frac{(\Gamma_>/2\pi)^{1/2}}{E - E'_> - i(\Gamma_>/2)}\left[|\zeta_>\rangle + \left(\frac{1}{2T_0+1}\right)^{1/2}\int \frac{|\xi_\epsilon^{(-)}\rangle\langle\xi_\epsilon^{(-)}|\Delta|\tilde{\Phi}_p^{(1)}\rangle d\epsilon}{E^{(-)} - \epsilon}\right]. \tag{24}$$

The solution demonstrates the occurrence of two resonances, which are readily recognized as the $T_<$ and $T_>$ analog resonances; the resonance energies $E'_<$ and $E'_>$ are shifted somewhat from the QHQ eigenvalues $E_<$ and $E_>$ by the usual shifts, but this is a minor point. The original single-proton resonance occurring close to the energy $E_<$ has now been aplit up. A fraction $[2T_0/(2T_0+1)]^{1/2}$ is contained in the $T_<$ resonance and a small fraction $(2T_0+1)^{-1/2}$ is contained in the $T_>$ IAR.

The splitting of the (nA) configuration between the two resonances is also evident. Finally, it is clear from Eq. (13) that the function $\xi^{(-)}$ will not display any resonances in the energy region of interest. We now project out the proton configuration of $\Psi^{(-)}$.

A comparison with the work of Garside and MacDonald[15] shows that if $2T_0 \gg 1$, the first two terms of Eq. (24), after projection, reconstruct the solution of Eq. (5) with $\Delta = 0$. We denote this solution by $\chi_E^{(-)}$. In other words, $\chi_E^{(-)}$ is the ordinary optical-model scattering solution for the proton channel. Thus,

$$\langle pC|\Psi_E^{(-)}\rangle = \chi_E^{(-)} + \frac{(\Gamma_>/2\pi)^{1/2}}{E - E'_> - i(\Gamma_>/2)}\frac{1}{(2T_0+1)^{1/2}}$$
$$\times\left[\tilde{\Phi}_p^{(1)} + \int \frac{\langle pC|\xi_\epsilon^{(-)}\rangle\langle\xi_\epsilon^{(-)}|\Delta|\tilde{\Phi}_p^{(1)}\rangle d\epsilon}{E^{(-)} - \epsilon}\right]. \tag{25}$$

Equation (25) shows that the proton component of the IAR is a superposition of the ordinary optical-model wave function and a contribution that resonates at $E'_>$.[13] Equation (25) displays several important features on which comment is required:

(1) The ratio of the resonance contribution to the usual optical-model continuum function is dependent on T_0. As T_0 becomes large the resonance contribution becomes insignificant, whereas $\chi_E^{(-)}$ is still the unattenuated optical-model amplitude.

(2) The second term in square brackets describes the coupling of a fragment of the bound-state $\tilde{\Phi}_p^{(1)}$ to the continuum $\xi^{(-)}$, due to the "deepening-potential" Δ. The fragment in question is contained in $\zeta_>$. The charge-exchange potential is responsible for the fragmentation, which leaves behind a fairly good single-particle resonance at $E'_<$.

An approximation to Eq. (25) in which a proton continuum wave function is made to resonate at $E'_>$ by adjustment of the parameters of a Woods-Saxon potential, and then the entire wave function is divided by $(2T_0+1)^{1/2}$, is clearly inadequate in most cases. Only for IAR well below the Coulomb barrier, with moderate values of T_0, would good agreement between the two methods be expected. Equations (24) and (25) elucidate the Lane model, and provide explicit expressions for the solutions of interest to us. These expressions, however, require a knowledge of the continuum functions $\xi_\epsilon^{(-)}$, which are solutions of (13). Computer codes for solving Eq. (13) are not in widespread use; therefore, from a practical point of view, it is desirable to use a different technique,[17] being guided by the results and insights obtained above.

The above solution suggests that we try a solution to H with the ansatz,

$$\Psi_E = u_{pE}(r)|pC\rangle + b(E)u_n(r)|nC\rangle, \tag{26}$$

where

$$u_{pE}(r) = \int a_E(\epsilon)\phi_\epsilon d\epsilon \tag{27}$$

and

$$\langle \phi_\epsilon | \phi_{\epsilon'} \rangle = \delta(\epsilon - \epsilon') . \tag{28}$$

The neutron component, however, satisfies the normalization

$$\langle u_n | u_n \rangle = 2T_0/(2T_0+1) . \tag{29}$$

In addition, ϕ_ϵ and u_n satisfy (5) and (8), respectively, with $\Delta = 0$. Following now a procedure similar to the one employed earlier,[13,17] we can straightforwardly solve for $b(E)$ and $a(\epsilon)$ to get

$$\Psi_E^{(-)} = \frac{\mathfrak{V}_\epsilon^*}{E - \mathcal{E}_A - i\Gamma/2} \left\{ |u_n\rangle |nA\rangle + \left[\int \frac{\mathfrak{V}_\epsilon \phi_\epsilon^{(-)} d\epsilon}{E^{(-)} - \epsilon} \right] |pC\rangle \right\} + \phi_E^{(-)} |pC\rangle . \tag{30}$$

Here we have defined

$$\mathfrak{V}_\epsilon^* = \langle u_n | \sqrt{\tfrac{1}{2}T_0}\, V_1 | \phi_\epsilon^{(-)} \rangle , \quad \Gamma = \Gamma_E = 2\pi |\mathfrak{V}_E|^2 . \tag{31}$$

The resonance energy of the IAR is denoted by $\mathcal{E}_A$. In evaluating the integral in (30) one must realize that both ϕ_ϵ and $\mathfrak{V}_\epsilon$ display a very strong energy dependence due to the proton single-particle resonance at an energy which we denote by $E_{s.p.}$. This energy is far below the Coulomb barrier and the width of the single-particle resonance is extremely small (for the cases for which we perform numerical calculations, the width is of the order of electron volts or less). In a small neighborhood surrounding the energy $E_{s.p.}$, we may write

$$\phi_E \cong \Phi_n \frac{(\gamma/2\pi)^{1/2}}{[(E - E_{s.p.})^2 + \gamma^2/4]^{1/2}} . \tag{32}$$

Here γ denotes the width of the single-particle resonance. We also observe that

$$E_{s.p.} \cong \mathcal{E}_A - T_0 \langle \Phi_n | V_1 | \Phi_n \rangle . \tag{33}$$

Using Eqs. (32), (33), and (30) we get

$$\langle pC | \Psi_E^{(-)} \rangle = \frac{\mathfrak{V}_E^*}{E - \mathcal{E}_A - i\Gamma/2} \left[\frac{1}{(2T_0+1)^{1/2}} \Phi_n + \mathrm{P}' \int \frac{\mathfrak{V}_\epsilon \phi_\epsilon^{(-)} d\epsilon}{E - \epsilon} + \frac{E - \mathcal{E}_A}{\mathfrak{V}_E^*} \phi_E^{(-)} \right] \tag{34}$$

or

$$\langle pC | \Psi_E^{(-)} \rangle = \frac{\mathfrak{V}_E^*}{E - \mathcal{E}_A - i\Gamma/2} \left[\frac{1}{(2T_0+1)^{1/2}} \Phi_n + \mathrm{P}' \int \frac{\mathfrak{V}_\epsilon \phi_\epsilon^{(-)} d\epsilon}{E - \epsilon} + i\pi \mathfrak{V}_E \phi_E^{(-)} \right] + \phi_E^{(-)} . \tag{35}$$

In (34) and (35), P′ indicates that in evaluating the principal value integral the contributions from the proton single-particle resonance are to be deleted.

Equation (35) again shows that the proton wave function of the IAR consists of a superposition of the normal optical-model solution and a resonating contribution. In the next section, we calculate the DWBA amplitude for the proton stripping reaction using Eq. (34). It is clear from the form of this result that we have a nonresonant contribution due to $\phi_E^{(-)}$ which varies smoothly with the energy of the emitted proton, and a resonance contribution which gives rise to a peak in the observed cross section at the proton energy $\mathcal{E}_A$. If the two amplitudes are of comparable magnitude, we expect interference terms to be important.

The discrete neutron groups observed in a (d,n) reaction to IAR in intermediate to heavy nuclei sit on a "background" which is, at least in large part, a neutron continuum from (d,np) breakup. Since this "background" is simply subtracted away in reducing the (d,n) data, the theoretical quantity corresponding to the measured cross section is the difference between the cross section

$$\iint_\Delta \frac{d^3\sigma}{d\Omega_n d\Omega_p dE_n} dE_n d\Omega_p$$

computed with Eq. (35) as the form factor, and the three-body breakup cross section computed with $\phi_E^{(-)}$ only as the form factor. Here Δ is the experimental width of the neutron group which is summed over. Similar comments apply to the available $(^3\mathrm{He}, d)$ data. We would like to choose cases for analysis in which the resonant contribution to Eq. (35) is predominant, so that we can avoid the full complexity of a three-body breakup calculation and use the ordinary DWBA insofar as is possible. The data[7-9] indicate that for many transitions the resonance amplitude dominates. In view of this, we approximate Eq. (34) by deleting the last term in the square bracket; thus,

$$\chi_p^{(R)} \equiv \langle pC | \Psi^{(-)} \rangle \cong \frac{\mathfrak{V}_E^*}{E - \mathcal{E}_A - i\Gamma/2} \left[\frac{1}{(2T_0+1)^{1/2}} \Phi_n + \mathrm{P}' \int \frac{\mathfrak{V}_\epsilon \phi_\phi^{(-)} d\epsilon}{E - \epsilon} \right] . \tag{36}$$

III. DWBA CROSS SECTION

We write the cross section for an $A(d,n)B^*$ reaction to the continuum states of B^* within dE_p of E_p, when the neutron is observed in the solid angle element $d\Omega_n$, and the decaying proton is not detected, as[1,2]

$$\frac{d^2\sigma}{d\Omega_n dE_p} = \frac{M_{nB} M_{pA} M_{dA}}{\pi^2 \hbar^6 k_d^3 k_p k_n} \left(\frac{B}{A}\right)^2 \frac{2J_B+1}{2J_A+1} \times \sum_{j m m_a m_b} \Big| \sum_{ls} C_{lsj} \beta_{lsj}^{m m_a m_b} \Big|^2 , \tag{37}$$

using the notation of Bunakov[2] and Satchler.[18] $\beta_{lsj}^{m m_a m_b}$ contains the radial overlap integral[18]

$$f_{L_n J_n L_d J_d}^{lsj} = \int \chi_{L_n J_n} \left(\frac{A k_n r}{B}\right) \frac{\chi_{lsj}(r)}{r} \chi_{L_d J_d}(k_d r) dr , \tag{38}$$

where $\chi_{LJ}(kr)$ is the L,Jth radial partial wave corresponding to $\chi^{(+)}(\vec{k},\vec{r})$. For stripping to the continuum, $\chi_{lsj}(r)$ is assumed in Eq. (37) to carry the usual factor $(4\pi/k_p r)$. In fact, in Eqs. (34) and (35), we choose the continuum energy normalization so that Eq. (38) must be multiplied by $(k_p/\pi E_p)^{-1/2}$. Thus Eq. (37) becomes

$$\frac{d^2\sigma}{d\Omega_n dE_p}=\frac{M_{nB}M_{dA}}{2\pi\hbar^4 k_d^3 k_n}\left(\frac{B}{A}\right)^2\frac{2J_B+1}{2J_A+1}\times\sum_{jmm_am_b}\left|\sum_{ls}C_{lsj}\beta_{lsj}^{mm_am_b}\right|^2, \tag{39}$$

which is identical in form to the usual DWBA cross section.[18] Since we deal with cases in which a single sharp resonance dominates the proton continuum, the sums on j, l, and s can be omitted.

Many writers have discussed the poor convergence of the overlap integral, Eq. (38), when $\chi_{lsj}(r)$ is a continuum function. The standard method of evaluating Eq. (38) under such conditions was suggested by Huby and Mines[19] and has been widely used. Studies of the validity of the approach have been made by Berggren[20] and by Vincent.[21] One simply inserts a convergence factor, $e^{-\alpha r}$ or $e^{-\beta r^2}$, into Eq. (38) and extrapolates to α or $\beta=0$. Such weight functions have also been used to "normalize" continuum form factors.[20,22]

Alternate approaches have been discussed by Bunakov[2,23] and by Vincent and Fortune.[3] The general validity of the "surface integral" method of Bunakov is difficult to establish without extensive numerical tests, but so far[23] it does not appear necessarily more stable than the Huby-Mines method. The contour-integration approach of Vincent and Fortune has been applied mainly to (d,p) and (d,n) for light targets,[3] but is clearly generally useful. We adopt the Huby-Mines procedure, for simplicity only.

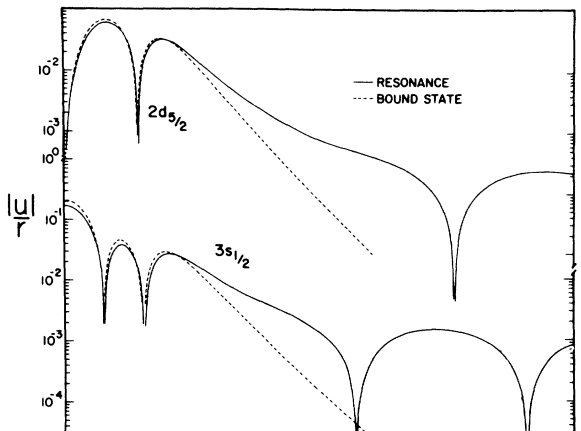

FIG. 1. Comparison of parent bound-state (^{93}Mo, dashed line) and IAR (^{93}Tc^A, solid line) form factors for the $2d_{5/2}$ and $3s_{1/2}$ states. The parent bound-state functions were computed by the separation-energy procedure in a Woods-Saxon potential with parameters $r_0=1.24$ fm, $a_0=0.65$ fm, $V_{so}=6.25$ MeV. The resonance form factors were computed from Eq. (42) using the same parameters, with $V_1=1.34$ MeV.

The procedure of Huby and Mines has one further advantage beyond simplicity, namely that the stability and reliability of the result is simple to study by variation of α, the DWBA outer cutoff radius R_c, and the number of partial waves. We find that the procedure works well for the narrow resonances considered here for the (d,n) case at 12-MeV incident deuteron energy.[8]

As $\chi_{lsj}(r)$ in Eq. (38), we use Eq. (36). After integration of the cross section over a proton energy interval $\gg\Gamma$, we obtain to a good approximation

$$\frac{d\sigma}{d\Omega_n}=\frac{M_{nB}M_{dA}}{2\pi\hbar^4 k_d^3 k_n}\left(\frac{B}{A}\right)^2\frac{2J_B+1}{2J_A+1}\sum_{mm_am_b}|C_{lsj}\tilde{\beta}_{lsj}^{mm_am_b}|^2, \tag{40}$$

where $\tilde{\beta}$ depends upon

$$f_{L_nJ_nL_dJ_d}^{lsj}=\int\chi_{L_nJ_n}\left(\frac{Ak_n r}{B}\right)\tilde{\chi}_{lsj}(r)\chi_{L_dJ_d}(k_d r)\frac{dr}{r}, \tag{41}$$

with

$$\tilde{\chi}_{lsj}(r)=(2T_0+1)^{-1/2}\Phi_n(r)+P'\int\frac{v_\epsilon\phi_\epsilon^{(-)}d\epsilon}{E_A-\epsilon}. \tag{42}$$

It is instructive to compare $\tilde{\chi}_{lsj}$ to the approximation $\chi_p^R\approx\chi_p^A$. This is done in Fig. 1 for the $d_{5/2}$ and $s_{1/2}$ IAR in ^{93}Tc^A.

We stress that Eq. (40) is the cross section for population of the IAR, assuming that the neutron peak in the time-of-flight spectrum is summed conventionally (i.e., we have integrated over the energy spread due to population of an IAR rather than a particle-bound state). Because in ^{93}Tc^A we deal with a case in which the elastic or proton channel is the only significant mode of decay, the spreading of the IAR due to mixing with its surrounding $T_<$ continuum will not affect the energy-integrated cross sections considered here.

One may well be interested experimentally and theoretically in the precise line shape of the (d,n) neutron group. In such a case it is necessary to do a detailed calculation of

$$\int\frac{d^3\sigma}{d\Omega_n d\Omega_p dE_n}d\Omega_p.$$

Such a calculation will require careful treatment of the spreading of the IAR into the $T_<$ states. Inclusion of such effects in the framework of an ap-

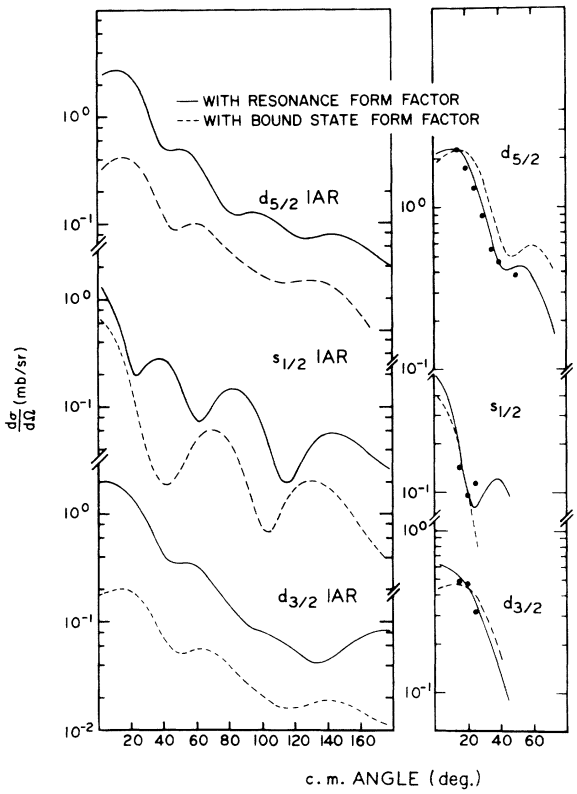

FIG. 2. Comparison of DWBA angular distributions for ^{92}Mo$(d,n)^{93}$Tc^A at E_d = 12 MeV, leading to the $d_{5/2}$, $s_{1/2}$, and $d_{3/2}$ IAR. The dashed line shows the usual DWBA cross section using as form factor approximation (A). The solid line shows the cross section using Eq. (42) and the Huby-Mines convergence procedure. Optical parameters are given in the text. On the right, the angular distributions are compared with the data of Ref. 8. The $d_{5/2}$ spectroscopic factor is 0.87.

proach to IAR similar in spirit to ours, but more general, has been discussed by Bledsoe and Tamura.[24]

Finally we point out that no qualitative arguments[3] are required to define a spectroscopic factor when the shell-model theory of reactions is used to compute the resonance form factor, since the usual spectroscopic amplitude $(S_{lj})^{1/2}$ is carried by $\Phi_n(r)$, which appears in every term of Eq. (42). Thus, not only does Eq. (40) have the same form as the usual DWBA cross section, but $C_{lsj} = S_{lj}{}^{1/2} D_0$ has the same meaning as for ordinary (d,n) reactions. We take the zero-range factor $D_0{}^2 = 1.48 \times 10^4$ MeV^2 fm^3 in the calculations reported here.

IV. NUMERICAL RESULTS

Our example is ^{92}Mo$(d,n)^{93}$Tc^A populating the $d_{5/2}$ IAR at 8.40 MeV, the $s_{1/2}$ IAR at 9.33 MeV, and the $d_{3/2}$ IAR at 9.91 MeV in ^{93}Tc. The partial proton and total widths of these resonances, which occur at laboratory proton energies of 4.36, 5.31, and 5.89 MeV are, respectively, ~1 keV, ~20 keV; 12 keV, 41 keV; 3 keV, 27 keV.[25] The spectroscopic factors of the parent neutron states from (d,p) are 0.84, 0.64, and 0.50.[26]

In Fig. 1, we compare the proton form factors computed using Eq. (36) with the corresponding bound-neutron functions of the parent states in ^{93}Mo, for $d_{5/2}$ and $s_{1/2}$. It is seen that the form factors agree quite well within the nuclear interior, but become appreciably different beyond the nuclear surface. Since it is the surface region which makes the predominant contribution to the DWBA amplitude in general, a difference in the detailed shape and magnitude of the cross section is expected. At large distances, 30–40 F, the bound-state form factor becomes negligible, while the resonance form factor oscillates with a small (10^{-3}) amplitude, relative to its interior values.

A convergence function $e^{-\alpha r}$ was used with the minimum value of α in the extrapolation to $\alpha = 0$ taken as $\alpha \leq 10/R_c$ fm^{-1}, where R_c is the outer cutoff radius. R_c was varied from 40 to 100 fm to test the stability of the extrapolated result. The cross section for the two $l = 2$ transitions was constant to within a few percent during all variations.

In Fig. 2 are shown the results of the calcula-

TABLE I. ^{92}Mo$(d,n)^{93}$Tc^A theoretical and experimental cross sections (in mb/sr) at 25° lab.

IAR	Method	$(d\sigma/d\Omega)_B$ [a] $S=1$	$(d\sigma/d\Omega)_B$ [a] $S=S_{dp}$	$(d\sigma/d\Omega)_R$ [b] $S=1$	$(d\sigma/d\Omega)_R$ [b] $S=S_{dp}$	$(d\sigma/d\Omega)_{SPR}$ [c]	$(d\sigma/d\Omega)_{EXP}$ [d]
$d_{5/2}$, 4.32 MeV	L	0.469	0.393	1.895	1.591	2.20	1.3 ±0.2
(S_{dp}=0.84)	NL	0.351	0.294	1.867	1.568		
$s_{1/2}$, 5.25 MeV	L	0.136	0.087	0.219	0.140	0.130	0.12±0.04
(S_{dp}=0.64)	NL	0.076	0.048	0.256	0.163		
$d_{3/2}$, 5.83 MeV	L	0.213	0.106	1.131	0.565	0.750	0.32±0.05
(S_{dp}=0.50)	NL	0.166	0.083	1.139	0.569		

[a] Using approximation (A).
[b] Using Eq. (42).
[c] Calculations of Ref. 10.
[d] See Ref. 8; and J. Horton, private communication.

TABLE II. ^{92}Mo$(d,n)^{93}$Tc^A theoretical and experimental cross sections (in mb/sr) at 15° lab.

IAR	Method	$(d\sigma/d\Omega)_B$ [a] $S=1$	$(d\sigma/d\Omega)_B$ [a] $S=S_{dp}$	$(d\sigma/d\Omega)_R$ [b] $S=1$	$(d\sigma/d\Omega)_R$ [b] $S=S_{dp}$	$(d\sigma/d\Omega)_{EXP}$ [c]
$d_{5/2}$, 4.32 MeV	L	0.545	0.457	2.720	2.283	2.3 ±0.2
($S_{dp}=0.84$)	NL	0.408	0.342	2.662	2.236	
$s_{1/2}$, 5.25 MeV	L	0.459	0.239	0.665	0.425	0.14 ±0.04
($S_{dp}=0.64$)	NL	0.287	0.183	0.525	0.336	
$d_{3/2}$, 5.83 MeV	L	0.237	0.118	1.664	0.832	0.48 ±0.05
($S_{dp}=0.50$)	NL	0.197	0.098	1.708	0.854	

[a] Using approximation (A).
[b] Using Eq. (42).
[c] See Ref. 8; and J. Horton, private communication.

tions. The dashed line is the angular distribution for each transition, with a bound-state form factor $(2T_0+1)^{-1/2}\Phi_n(r)$, as in approximation (A). The solid line is the angular distribution computed using Eq. (42). Normalization is absolute.

The optical parameters used in these calculations, in a standard notation, are: deuteron channel, $V=88.0$ MeV, $W_D=14.0$ MeV, $V_{so}=6.0$ MeV, $r_0=1.281$ fm, $a_0=0.727$ fm, $r'=1.41$ fm, $a'=0.694$ fm, $r_{so}=1.20$ fm, $a_{so}=0.687$ fm, $r_C=1.3$ fm; neutron channel, $V=48$ MeV, $W_D=8.1$ MeV, $V_{so}=7.0$ MeV, $r_0=r'=r_{so}=1.27$ fm, $a_0=a_{so}=0.66$ fm, $a'=0.47$ fm. These parameters are taken from optical-model analyses reported by Coker and Tamura,[27] and Clarkson and Coker.[28] The program VENUS, by Tamura,[29] was used with an outer cutoff of up to 100 fm. A Perey nonlocality correction was made using $\beta_d=0.65$ fm and $\beta_n=0.85$ fm, for the calculations shown in Fig. 2.

The right-hand strip of Fig. 2 shows a comparison of the predicted angular distributions with revised data of Ref. 8 (private communication from J. Horton). It is seen, particularly for the $d_{5/2}$ transition where there is a reasonable range of data, that the angular distributions computed with the bound-state form factor do not have the proper slope at forward angles, whereas the angular distributions computed with the resonance form factors are consistent with the available data.

Finally, in Tables I and II are shown the numerical results of the calculations. It is seen that with or without a nonlocality correction the magnitude of the calculated angular distributions is in remarkable agreement with experiment using Eq. (42), but that approximation (A) fails to account for the magnitude of the observed cross section for the $l=2$ transitions by factors of 3 to 5.

Since these calculations were completed, a Letter by Cole, Huby, and Mines[10] has appeared in which these same data were fit using potential resonance form factors to describe the IAR. The results of these calculations are given in Table I as $(d\sigma/d\Omega)_{SPR}$, for comparison. It is seen that the use of Eq. (42) gives considerably better results.

V. CONCLUSIONS AND SUMMARY

We have shown how to obtain a form factor for proton transfer reactions populating IAR, using an approach which readily generalizes to include many open channels and isospin mixing with the $T_<$ spectrum. For the example of ^{92}Mo$(d,n)^{93}$Tc^A to three prominent IAR, we have shown that IAR form factors calculated according to the methods outlined in Sec. II give relative cross sections in good agreement with experiment when the Huby-Mines procedure is used to produce convergence of the DWBA amplitude. In further work, use of the approach of Vincent and Fortune would be more suitable in obtaining convergence. Direct solution of Eq. (13) by iteration would also be of interest in constructing the exact expression (25), as an alternative to Eq. (35) used in the present work.

ACKNOWLEDGMENTS

The authors acknowledge the help of R. D. Alders and J. L. Horton in performing many numerical calculations, that formed the basis of approximations, mentioned in Sec. II. We also acknowledge helpful discussions with C. F. Moore, P. Richard, F. Rybicki, and T. Tamura.

*Work supported in part by the U. S. Atomic Energy Commission.

[1] F. S. Levin, Ann. Phys. (N.Y.) 46, 41 (1968).
[2] V. E. Bunakov, Nucl. Phys. A140, 241 (1970).
[3] C. M. Vincent and H. T. Fortune, Phys. Rev. C 2, 782 (1970).
[4] R. Huby, Phys. Letters 33B, 323 (1970).
[5] H. Fuchs, K. Grabish, and G. Röshert, Nucl. Phys.

A129, 545 (1969).
[6]W. Bohne, D. Hilcher, H. Homeyer, H. Morgenstern, and J. A. Scheer, Nucl. Phys. A106, 442 (1968).
[7]R. L. McGrath, N. Cue, W. R. Hering, L. L. Lee, B. L. Liebler, and Z. Vager, Phys. Rev. Letters 25, 682 (1970).
[8]S. A. A. Zaidi, C. L. Hollas, J. L. Horton, P. J. Riley, J. C. L. Ford, and C. M. Jones, Phys. Rev. Letters 25, 1503 (1970).
[9]D. H. Youngblood, R. L. Kozub, R. A. Kenefick, and J. C. Hiebert, Phys. Rev. C 2, 477 (1970); see also R. L. Kozub and D. H. Youngblood, Bull. Am. Phys. Soc. 15, 1657 (1970).
[10]B. J. Cole, R. Huby, and J. R. Mines, Phys. Rev. Letters 26, 264 (1971).
[11]A.M. Lane, Nucl. Phys. 35, 676 (1962).
[12]P. E. Hodgson and J. R. Rook, Nucl. Phys. 37, 632 (1962).
[13]H. Feshbach, Ann. Phys. (N.Y.) 5, 357 (1958); 19, 287 (1962).
[14]T. Tamura, Phys. Rev. 185, 1296 (1969).
[15]L. Garside and W. M. MacDonald, Phys. Rev. 138, B582 (1965).
[16]D. Robson, Phys. Rev. 137, B535 (1965).
[17]U. Fano, Phys. Rev. 124, 1866 (1961).
[18]G. R. Satchler, Nucl. Phys. 55, 1 (1964).
[19]R. Huby and S. R. Mines, Rev. Mod. Phys. 37, 406 (1965).
[20]T. Berggren, Nucl. Phys. A109, 265 (1968).
[21]C. M. Vincent, Phys. Rev. 175, 1309 (1968).
[22]J. Bang and J. Zimanyi, Nucl. Phys. A139, 534 (1969).
[23]V. C. Bunakov, K. A. Gridnev, and L. V. Krasnov, Phys. Letters 32B, 587 (1970).
[24]H. Bledsoe and T. Tamura, Nucl. Phys. A164, 191 (1971).
[25]C. F. Moore, P. Richard, C. E. Watson, D. Robson, and J. D. Fox, Phys. Rev. 141, 1166 (1966).
[26]J. B. Moorehead and R. A. Moyer, Phys. Rev. 184, 1205 (1969).
[27]W. R. Coker and T. Tamura, Phys. Rev. 184, 1277 (1969).
[28]R. G. Clarkson and W. R. Coker, Phys. Rev. C 2, 1108 (1970).
[29]T. Tamura and C. E. Watson, Phys. Letters 25B, 186 (1967); T. Tamura, W. R. Coker, and F. Rybicki, to be published.

PHYSICAL REVIEW C VOLUME 4, NUMBER 1 JULY 1971

New $K^\pi = 8^-$ Isomer in ^{182}Hf†

T. E. Ward and P. E. Haustein
Chemistry Department, Brookhaven National Laboratory, Upton, New York 11973
(Received 24 March 1971)

A new β active $K^\pi = 8^-$ isomer of 9×10^6-yr ^{182}Hf has been produced via the reaction ^{186}W-$(p,p\alpha)^{182m}$Hf. 14 γ rays have been observed to follow a half-life of 65 ± 5 min. Six of the transitions result from the deexcitation of a $K^\pi = 8^-$ isomeric level in ^{182}Hf at 1173.5 keV to members of the $K^\pi = 0^+$ ground-state rotational band. The decay of this new K isomer is discussed in relation to the well-known decay of 5.5-h ^{180m}Hf to which it is remarkably similar.

A number of isomeric states have been found[1,2] in the mass range $A = 176$–184. The $N = 106$ isotones ^{176}Yb, ^{178}Hf, ^{180}W, ^{182}Os, ^{184}Pt and the additional Hf isomers at masses 176 and 180 have been interpreted[3] as $K^\pi = 8^-$ two-quasiparticle states with probable Nilsson configurations of $\frac{7}{2}^-[514]_n$, $\frac{9}{2}^+[624]_n$ or $\frac{7}{2}^+[404]_p$, $\frac{9}{2}^-[514]_p$.

In the present investigation a new 65 ± 5-min γ-ray activity assigned to ^{182m}Hf was observed in the Hf fraction from targets of tungsten metal or isotopically enriched $^{186}WO_3$ (97%) that were irradiated with 33- or 50-MeV protons. Cross sections for the production reactions at these energies were estimated to be ~5 μb. The radiochemical separation of Hf from irradiated tungsten targets consisted of three main decontamination steps: (a) precipitation of hafnium from HF solutions as $BaHfF_6$; (b) extraction of hafnium into 0.5 M TTA in xylene, with back extraction into 0.5 N HNO_3-0.5 N HF solution; and (c) the final precipitation as hafnium tetramandelate with mandelic acid. The sources of hafnium obtained were highly decontaminated from neighboring elements. Chemical yields of about 60% were obtained in separation times of 40–60 min. The sources were counted with commercially available Ge(Li) detectors which had been calibrated for energy and efficiency with International Atomic Energy Agency standard sources. Analysis of the γ-ray spectra was performed by means of a modified version of the BRUTAL[4] computer code. The CLSQ[5] program was used for decay-curve resolutions.

In Table I are listed the γ-ray energies and relative intensities for ^{182m}Hf. The values for 5.5-h ^{180m}Hf are listed for comparison. Least-squares analysis of the more intense lines yielded a 65 ± 5-min half-life. All γ rays assigned to ^{182m}Hf decayed with approximately this half-life.